ELSEVIER

Computational Materials Science 2 (1994) 468–474

COMPUTATIONAL MATERIALS SCIENCE

Modifying the buckyball

David Tománek

Department of Physics and Astronomy and Center for Fundamental Materials Research, Michigan State University, East Lansing, MI 48824-1116, USA

(Received 8 August 1993; accepted 26 January 1994)

Abstract

Structural and electronic properties of carbon clusters, in particular the C_{60} "buckyball" molecule as well as structurally and chemically modified fullerenes, are calculated using a combination of predictive ab initio techniques and parametrized total energy schemes. These calculations indicate that single- and multi-shell fullerenes are the most stable C_n isomers at $T = 0$ for $n < 20$. More open structures are favored by entropy at higher temperatures. Upon interaction with donor elements, C_{60} molecules form stable $M@C_{60}$ endohedral complexes; analogous acceptor-based complexes are unstable. Solid C_{60} reacts with alkali metals and forms a stable intercalation compound which shows superconducting behavior. The relatively high value of the critical temperature for superconductivity can be explained quantitatively within the Bardeen–Cooper–Schrieffer formalism.

1. Introduction

The discovery of the C_{60} molecule [1] and successful development of a mass production technique for this system [2] has triggered a world-wide interest in this novel form of carbon. The resulting research effort first concentrated on characterizing this molecule and the corresponding solid. Next, spurred by the discovery of superconductivity in the alkali intercalated C_{60} solid [3,4], substantial effort has been invested in modifying the C_{60} molecule and solid. Ongoing research focuses both on the structural and electronic properties of C_{60}-inspired carbon fullerenes. At present, the most intensively investigated systems are multi-shell fullerenes ("bucky onions") [5], endohedral fullerene complexes containing encapsulated atoms [6], and exohedral solid C_{60} intercalation compounds containing intercalant atoms in the interstitial sites.

In the following, I will first address the stability and growth mechanism of C_{60} "buckyballs" and related fullerenes. These results are crucial for the understanding of the optimum conditions for the synthesis of C_{60}. Next, I will discuss the origin of superconductivity in the intercalated C_{60} solid. Understanding the pairing mechanism may lead to a possible design of novel C_{60} based high-temperature superconductors. Finally, I will turn to the stability of multi-shell fullerenes and fullerene endohedral complexes, promising candidates for novel molecules with tailored properties. I will show that presently available ab initio techniques can provide quantitative answers to most of the above points. Nevertheless, it appears equally important to isolate the essential physics and to find good models which generalize the results to other systems.

SSDI 0927-0256(94)00012-2

2. Theoretical tools

2.1. Density functional formalism

One of the most powerful tools in the calculation of complex systems such as modified buckyballs is the density functional theory (DFT) [7]. It is built on the Kohn–Sham theorem stating that in the ground state, the total electronic energy for a given system is a unique functional of the total charge density $\rho(r)$. The physical charge density can be obtained by minimizing this functional, given by

$$E[\rho] = T_0[\rho] + \int \mathrm{d}r\, \rho(r) V_{\mathrm{ext}}(r) + E_{\mathrm{H}}[\rho] + E_{\mathrm{xc}}[\rho] = \min. \quad (1)$$

Here, T_0 is the kinetic energy functional, $V_{\mathrm{ext}}(r)$ is the potential of the ions, $E_{\mathrm{H}}[\rho]$ is the Hartree and $E_{\mathrm{xc}}[\rho]$ is the exchange–correlation functional. This technique is parameter-free. The knowledge of atomic numbers and atomic positions is sufficient to determine the total energy and the electron density $\rho(r)$ of a given system. The minimization of the energy functional given in Eq. (1) is achieved by solving self-consistently the set of Kohn–Sham equations

$$(-\tfrac{1}{2}\nabla^2 + V_{\mathrm{ext}} + V_{\mathrm{H}} + V_{\mathrm{xc}})\psi_{nk} = \epsilon_{nk}\psi_{nk},$$

$$\rho(r) = \sum_{nk}^{\mathrm{occ}} |\psi_{nk}(r)|^2. \quad (2)$$

In the local density approximation (LDA), the nonlocal functional $E_{\mathrm{xc}}[\rho]$ is replaced by a local function $\tilde{E}_{\mathrm{xc}}(\rho)$ which reproduces the exchange–correlation energy in the homogeneous electron gas exactly. We replace the ionic potentials by first-principles pseudopotentials, which combine the nucleus and core electrons, and use a local Gaussian orbital basis. Yet even with these simplifications, ab initio DFT calculations are computationally very intensive. For this reason, many parametrized techniques compete successfully with this formalism.

2.2. Tight-binding formalism

In a one-electron picture, the total energy of a carbon cluster can be obtained using the expression [8]

$$E_{\mathrm{tot}} = \sum_{\alpha} n_\alpha \epsilon_\alpha + \sum_{i<j} E_{\mathrm{r}}(d_{ij}) + \sum_i \psi(Z_i) + U \sum_{i=1}^{n} (q_i - q_i^0)^2. \quad (3)$$

Here, the electronic states of the cluster have been labeled by α and the atomic sites by i, j. The first term in Eq. (3) is the one-electron energy of the cluster, obtained using a Slater–Koster parametrized tight-binding Hamiltonian. The second and third term describe nuclear repulsion and electronic "overcounting" terms, which are represented by pairwise repulsive energies $E_{\mathrm{r}}(d)$ and correction terms for highly coordinated structures with coordination numbers Z_i. The final fourth term is an intra-atomic Coulomb repulsion arising from possible charge transfer between inequivalent sites.

The input information consists of the atomic positions and the tight-binding parameters. The information available as output is the total energy of the system E_{tot}, the molecular orbital wave functions, and the energy eigenvalues ϵ_α. The tight-binding parameters have been obtained from a fit to LDA results for C_2, graphite and diamond, and are given in Ref. [8]. This formalism is computationally very efficient, and is ideally suited to determine equilibrium structural and electronic properties of large carbon systems, as well as for molecular dynamics simulations.

3. Applications

In the following, I will show how this formalism can be applied to carbon clusters, in particular the C_{60} buckyballs and the C_{60} solid [9]. The C_{60} cluster is the most spherical molecule known: it is a hollow cage with a radius of ~ 3.5 Å, formed by 60 identically equivalent carbon atoms. The valence charge is delocalized across

the surface of the cage, strongly reminiscent of the charge density in a graphite monolayer. This is a consequence of the graphitic sp^2-type bonding in the C_{60} molecule. These strong covalent bonds are responsible for the structural stiffness of this molecule.

The C_{60} solid, sometimes called "fullerite", is a bulk structure obtained by stacking buckyballs. The equilibrium structure at room temperature is a face-centered cubic crystal. The bonding between individual C_{60} molecules is weakly covalent and van der Waals type, very similar to the weak inter-layer bonds in graphite.

3.1. *Formation of fullerenes*

In the following, I will discuss the abundancy of closed-shell fullerene structures, in particular the C_{60} "buckyball", both at $T = 0$ and at $T > 0$.

3.1.1. $T = 0$ *calculations*

The equilibrium structures of carbon clusters at $T = 0$ can be determined efficiently using the tight-binding Hamiltonian and the simulated annealing technique [8]. The equilibrium geometries, which were obtained in this procedure, included chains, rings, and hollow fullerene cages. For the sake of comparison, we also considered fullerene caps (fragments of a C_{60} molecule) and graphite flakes.

Our results, shown in Figs. 1a and 1b, indicate an increasing binding energy per atom with increasing cluster size. Based on these total energy results, which are relevant at $T = 0$, the most stable C_n isomers were found to be chains and rings for $n < 20$. At larger cluster sizes, in particular at $n > 20$, we expect and find rings to be more favorable than chains, since releasing the dangling bond energy of a chain easily offsets the bending energy when forming a ring. At these larger sizes, however, higher coordinated structures turn out to be energetically much more favorable. For $n > 20$, we find the hollow fullerenes to be the most stable isomers. We also find a gradual increase of the binding energy per atom with increasing fullerene size. Since in thermodynamic equilibrium the relative abundancy of different clusters should reflect their stability, our results would suggest a continuous size distribution of carbon fullerenes in the mass spectra. Hence we conclude that $T = 0$ calculations cannot explain the abundancy of the "magic" C_{60} cluster in the mass spectra.

3.1.2. $T > 0$ *calculations*

Since the standard arc synthesis process [2] of C_{60} involves high temperatures, we decided to investigate the stability of closed fullerene cages at high temperatures with respect to other open structures [10]. For a given temperature and cluster size, the most stable isomer is expected to have the lowest free energy. We determined the free energy F of a cluster from its total partition function Z, as

$$\begin{aligned} F &= -kT \ln Z \\ &= -kT(\ln Z_t + \ln Z_r + \ln Z_v + \ln Z_e \\ &\quad + \ln Z_s). \end{aligned} \tag{4}$$

Here, we took into account translational, rotational, vibrational and electronic degrees of freedom on top of a structural term which reflects the internal energy.

For the C_{20} system, we considered a chain, a ring, the smallest fullerene cage (a dodecahedron), and a corannulene cap structure (a fragment of the C_{60} molecule). We found that at $T = 0$, the most stable structure is the fullerene cage, closely followed by the cap, the ring, and the chain. With increasing temperature, the free energy of all these structures decreases. We find that the free energy of more open structures with softer vibrational degrees of freedom decreases faster, due to the importance of vibrational entropy. In particular, the corannulene cap becomes more stable than the C_{60} cage at a temperature of a few thousand Kelvin. We conclude that this and similar structures might be the precursors for C_{60}. These cap fragments are the most stable structures at high temperatures, and at the same time are the natural seeds for the growth of larger fullerenes such as C_{60}.

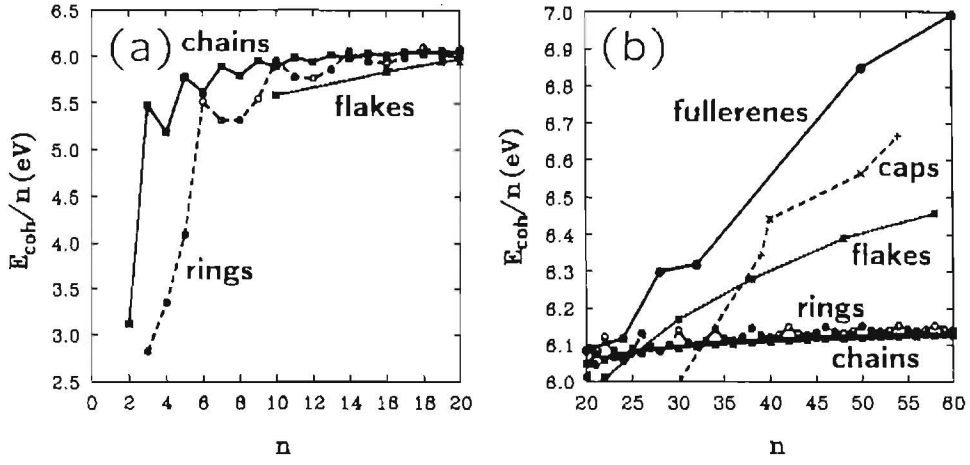

Fig. 1. Binding energy E_{coh} of small carbon clusters as a function of cluster size n, (a) for $n \leq 20$ and (b) for $n \geq 20$. Results for chains (□) are connected by a solid line, results for rings (○) are connected by a dashed line, and results for planar graphite flakes (*) are connected by a dotted line. Results for buckled fullerene caps with a pentagonal (×) or a hexagonal basis (+) are connected by a dashed line. Results for hollow fullerene cages (•) are connected by a solid line. (From Ref. [8], © American Physical Society.)

3.2. Superconductivity in the alkali doped C_{60} solid

Potentially the most important property of the C_{60} solid is its superconducting behavior when doped with alkali atoms [3,4]. In the following, I will present a quantitative Bardeen–Cooper–Schrieffer (BCS) theory which has been used successfully to describe the superconducting behavior of C_{60} [11]. The electronic states of the alkali doped M_3C_{60} solid are calculated using the LDA and the tight-binding formalism discussed above. The vibrational modes of the solid are determined using an extended Keating Hamiltonian which describes both on-ball and inter-ball vibrations.

McMillan's expression for the critical temperature for superconductivity T_c reads [12]

$$T_c = \frac{\hbar\omega_{log}}{1.2k_B} \exp\left[\frac{-1.04(1+\lambda)}{\lambda - \mu^* - 0.62\lambda\mu^*}\right]. \qquad (5)$$

In accordance with other standard superconductors, we used $\mu^* \approx 0.1$ for the effective Coulomb repulsion. The stiff on-ball vibrational modes of C_{60} yield $\hbar\omega_{log}/k_B \approx 1400$ K for the "Debye temperature" of the solid. With the electron–phonon coupling constant $\lambda \approx 0.6$, to be derived below, we can explain the observed value $T_c \approx 30$ K in Rb_3C_{60} [4].

The electron–phonon coupling constant is given by $\lambda = 2N(E_F)V$, where $N(E_F)$ is the electronic density of states at the Fermi level, and V is the Bardeen–Pines interaction which couples two electrons to a Cooper pair. The large value of λ is a consequence of both a large density of states at the Fermi level and a strong coupling of these states to vibrational states.

The conduction band is derived from the t_{1u} lowest unoccupied molecular orbital (LUMO) of C_{60}, and has p_π character. Due to the small inter-ball hopping, the width of this band is small, $W \approx 0.5$ eV [13,14]. For a featureless, e.g. rectangular, band, one can estimate $N(E_F) \approx 6/0.5\ \text{eV}^{-1} \approx 10\ \text{eV}^{-1}$. LDA calculations give $N(E_F) \approx 20\ eV^{-1}$ for a half filled band [13,14]. This density of states is at least one order of magnitude larger than that of intercalated graphite, consistent with the finding that T_c(intercalated graphite) $<<$ $T_c(M_3C_{60})$.

We used an extended Keating Hamiltonian, with parameters adjusted to reproduce the vibrational spectra of the C_{60} solid, to determine the vibrational eigenmodes of the crystal. For each of these modes, we investigated the cou-

pling to the conduction states. We found that coupling of the librational modes at $\nu \approx 10\ cm^{-1}$ can be neglected, while inter-ball optical modes at $\nu \approx 100\ cm^{-1}$ couple weakly. The important modes are on-ball modes at a frequency range $\nu \approx 200$–$1600\ cm^{-1}$. Among the most strongly coupling modes are the radial buckling H_g modes at $\nu \approx 400\ cm^{-1}$, the tangential pentagon breathing A_g mode at $\nu \approx 1600\ cm^{-1}$, and tangential optical H_g modes at $\nu \approx 1600\ cm^{-1}$. For these modes, we find $V \approx 21$ meV per C_{60}. The large values of V and of $N(E_F)$ yield a large electron–phonon coupling constant λ.

The dominant contribution of on-ball modes to the electron–phonon coupling makes it possible to treat electron–phonon coupling in relationship to a dynamical Jahn–Teller effect for the charged C_{60} molecule, and to consider solid C_{60} as a molecular crystal [15]. In this case, when changing the alkali intercalant M in M_3C_{60}, λ and consequently also T_c should only depend on the C_{60}–C_{60} separation which modifies $N(E_F)$. We expect an increase of T_c with an increasing lattice constant of M_3C_{60}, which is achieved by substituting a heavier alkali element M [14]. The same argument would lead to the conclusion that a reduction of the lattice constant, due to increasing pressure, should result in a reduction of T_c. Both these effects have been verified experimentally [14].

In conclusion, we found that standard BCS theory can provide a quantitative explanation for superconductivity in the alkali doped C_{60} solid. The observed large value of T_c is due to the high Debye temperature, a large value of $N(E_F)$, and a strong coupling of on-ball vibrational modes to states at E_F [11,14].

3.3. *Modified C_n fullerenes*

So far, we have been discussing the stability and synthesis of the C_{60} molecule, and properties of solids which contain this molecule as a building block. It is not difficult to imagine that other fullerene structures, inspired by C_{60}, could exhibit very interesting behavior. These "designer molecules" could be possibly optimized for a specific property, such as electron–phonon coupling in the solid. In the following, I will address the stability of two classes of such systems, namely multi-shell fullerenes and endohedral fullerene complexes.

3.3.1. *Bucky tubes and bucky onions*

A new type of graphitic structures, called "bucky tubes", has been observed in the apparatus used to produce C_{60} [16]. Electron microscopy images show that "bucky tubes", consisting of multiple graphitic shells, grow on the electrodes in the direction of the electric field. These structures are probably stabilized by a large polarization energy. On the other hand, irradiation of the carbon soot obtained in the Huffman–Krätchmer apparatus by an intense electron beam has yielded multi-shell spherical fullerenes consisting of up to several hundred of nested shells [5]. In both cases, the important question is, which are the most stable isomers for carbon structures containing hundreds and thousands of atoms.

In order to answer this question, we studied the stability of single- and multi-shell fullerenes with respect to graphite [17]. Among the prototype fullerene structures which we investigated were single- and multi-shell spheres, tubes and cones. In order to avoid dangling bond energies, we only considered closed surfaces, and terminated the single- and multi-shell tubes and cones at both ends by spherical caps.

Since even a parametrized tight-binding Hamiltonian is impractical to use at these large cluster sizes, we used continuum elasticity theory to determine the formation energy of these structures with respect to a graphite monolayer. For single-shell spherical fullerenes, we found that the total formation energy (with respect to a graphite monolayer) is independent of the cluster size. This finding could be quantitatively verified by plotting available data for carbon fullerenes with as few as 20–100 atoms. We also found that for a given number of atoms, a fullerene sphere is more stable than a cylinder or a cone. Based on the comparison between our continuum elasticity results and calculated formation energies of icosahedral fullerenes, the

relaxation from a perfect sphere to a polyhedron involves a sufficiently small energy which can be neglected in the further considerations.

The observation of multi-shell structures can be explained by the attractive, mainly van der Waals type, interaction between the shells, similar to the interlayer interaction in graphite. It is conceivable that for a sufficiently large cluster size, this inter-shell attraction outweighs the energy cost of producing multiple shells rather than one very large spherical fullerene. Our calculations indicate that for spheres, the transition from single-shell to multi-shell fullerenes occurs near $n \approx 700$ atoms. For extremely large structures with $n = 10^4$–10^6 atoms, we observe a scaling of the equilibrium number of shells, n_s, as $n_s \sim n^{1/3}$. The stability of these very large multi-shell fullerenes approaches asymptotically that of bulk graphite.

3.3.2. *Endohedral M@C$_{60}$ complexes*

The hollow space inside a C_{60} molecule is large enough to hold an atom. Buckyballs "stuffed" with the atom M, called M@C_{60} endohedral complexes, form an important class of modified buckyballs. We expect that these systems could be tailored to optimize the optical response of the free molecules or the critical temperature for superconductivity T_c when packed into a solid. The crucial issue to be addressed – prior to any speculations regarding their properties – is the stability of the endohedral complexes.

We decided to investigate the stability of M@C_{60} complexes using a thermodynamic Born–Haber cycle [18]. In this method, we decompose the formation energy ΔE_f of M@C_{60} from an isolated atom and an isolated C_{60} molecule into several energetically well defined steps. This is an exact procedure in the equilibrium state. Moreover, unlike the more involved ab initio calculations [19], this approach allows a simple interpretation of stability trends across the periodic table.

The Born–Haber cycle for a donor M@C_{60} complex is reproduced in Fig. 2. In the first step, we ionize the donor atom M, investing the ionization energy I(M), and put the extra charge

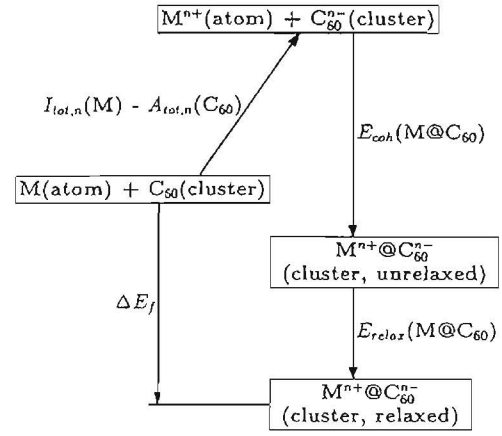

Fig. 2. Born–Haber cycle used to predict the formation energy ΔE_f of donor M@C_{60} endohedral complexes. (From Ref. [18], © Elsevier Science Publishers.)

onto the C_{60} molecule, gaining the electron affinity $A(C_{60})$. In the next step, we move the M ion into the middle of the negatively charged C_{60} cage. In this step, the system gains a considerable amount of Coulomb energy. This energy must be corrected for the energy needed to cross the dipole layer formed on the C_{60} surface, and for non-ionic M–C_{60} interactions. Finally, we let the M ion relax to an off-center position inside the C_{60} cage. In this step, the released polarization energy of the cage is partly compensated by a short-range M–C_{60} repulsion. This cycle is correct if the attractive M–C_{60} interaction is predominantly ionic, which is the case in most of the compounds considered, in analogy to graphite intercalation compounds. While the above Born–Haber cycle was presented explicitly for donor complexes, an analogous cycle can easily be constructed for an electron acceptor M, with the obvious modifications involving the electron affinity A(M) of M and the ionization potential $I(C_{60})$. We find the endohedral complex M@C_{60} to be stable when $\Delta E_f < 0$ and unstable when $\Delta E_f > 0$.

This decomposition of ΔE_f indicates that atom-specific properties enter mainly in the ionization potential (or electron affinity) of M. Our results indicate that stable complexes can be obtained with group IA elements, heavy elements

of group IIA, and early rare earth elements, all of them acting as donors. All investigated group VIA and group VIIA acceptor complexes were found to be unstable. The dominating factor determining the stability was found to be the ionization step. In general, the ionization energy of donor atoms is close to their electron affinity, $I(\text{donor M} \rightarrow \text{M}^+) \approx A(\text{acceptor M} \rightarrow \text{M}^-)$. For a C_{60} molecule, however, the ionization potential is much larger than the electron affinity. This is especially true for the higher ionization states, where $I(C_{60} \rightarrow C_{60}^{2+}) >> A(C_{60} \rightarrow C_{60}^{2-})$. Hence this ionization step is energetically much more costly for acceptor atoms than for donor atoms. Consequently, we find $\Delta E_f(\text{acceptor M}) > 0$ and $\Delta E_f(\text{donor M}) < 0$.

4. Summary and conclusions

I have discussed successful applications of both ab initio and parametrized techniques to quantitative calculations of the *stability* and *electronic properties* of carbon clusters, in particular carbon fullerenes and related systems.

At $T = 0$, the *equilibrium shapes* of free C_n clusters are chains and rings for $n < 20$, spherical fullerene cages for $n > 20$, and multi-shell onions for $n > 700$ atoms. Entropy is expected to play a significant role at $T > 0$. *Encapsulation* of atoms in free C_{60} "buckyball" molecules is energetically favorable for donor elements of groups IA and IIA, and unfavorable for acceptor elements of groups VIA and VIIA.

Superconductivity in the alkali doped C_{60} solid can be explained by the standard BCS theory. The important factors responsible for a large critical temperature T_c are a large electronic density of states at E_F and efficient coupling of conduction electrons by stiff on-ball modes.

Acknowledgements

This work has been performed in collaboration with George Bertsch, Jerzy Bernholc, Aurel Bulgac, Richard Enbody, Gregor Overney, Rodney S. Ruoff, Michael Schlüter, Yang Wang, and Weiqing Zhong, whose contributions are gratefully acknowledged. Financial support has been provided by the National Science Foundation under Grant No. PHY-9224745, the Air Force Office of Scientific Research under Grant No. F49620-92-J-0523DEF, and by the sponsors of the TAMC-1 conference.

References

[1] H.W. Kroto, J.R. Heath, S.C. O'Brien, R.F. Curl and R.E. Smalley, Nature 318 (1985) 162.
[2] W. Krätschmer, L.D. Lamb, K. Fostiropoulos and D.R. Huffman, Nature 347 (1990) 354.
[3] A.F. Hebard, M.J. Rosseinsky, R.C. Haddon, D.W. Murphy, S.H. Glarum, T.T.M. Palstra, A.P. Ramirez and A.R. Kortan, Nature 350 (1991) 600.
[4] M.J. Rosseinsky, A.P. Glarum, D.W. Murphy, R.C. Haddon, A.F. Hebard, T.T.M. Palstra, A.R. Kortan, S.M. Zahurak and A.V. Makhija, Phys. Rev. Lett. 66 (1991) 2830.
[5] D. Ugarte, Nature 359 (1992) 707.
[6] J.R. Heath, S.C. O'Brien, Q. Zhang, Y. Liu, R.F. Curl, H.W. Kroto and R.E. Smalley, J. Am. Chem. Soc. 107 (1985) 7779.
[7] P. Hohenberg and W. Kohn, Phys. Rev. 136 (1964) B864;
W. Kohn and L.J. Sham, Phys. Rev. 140 (1965).
[8] D. Tománek and M.A. Schluter, Phys. Rev. Lett. 67 (1991) 2331.
[9] Synthesis and topology of large fullerenes has been reviewed by R.F. Curl and R.E. Smalley, in: Scientific American (1991) p. 54.
[10] C.J. Brabec, E. Anderson, B.N. Davidson, S.A. Kajihara, Q.-M. Zhang, J. Bernholc and D. Tománek, Phys. Rev. BR46 (1992) 7326.
[11] M. Schluter, M. Lannoo, M. Needels, G.A. Baraff and D. Tománek, Phys. Rev. Lett. 68 (1992) 526.
[12] W.L. McMillan, Phys. Rev. 167 (1968) 331.
[13] S. Saito and A. Oshiyama, Phys. Rev. Lett. 66 (1991) 2637.
[14] M. Schlüter, M. Lannoo, M. Needels, G.A. Baraff and D. Tománek, J. Phys. Chem. Solids 53 (1992) 1473.
[15] M. Lannoo, G.A. Baraff, M. Schlüter and D. Tománek, Phys. Rev. BR44 (1991) 12106.
[16] S. Iijima, Nature 354 (1991) 56;
S. Iijima, T. Ichihashi and Y. Ando, Nature 356 (1992) 776.
[17] D. Tománek, W. Zhong and E. Krastev, Phys. Rev. B 48 (1993) 15461.
[18] Y. Wang, D. Tománek and R.S. Ruoff, Chem. Phys. Lett. 208 (1993) 79.
[19] J. Cioslowski and A. Nanayakkara, Phys. Rev. Lett. 69 (1992) 2871.